Wireless Pers Commun (2012) 65:293–318
DOI 10.1007/s11277-011-0250-6

Reverse Link Performance of DS-CDMA Cellular Systems through Closed-Loop Power Control, Base Station Assignment, and Antenna Arrays in 2D Urban Environment

Mohamad Dosaranian-Moghadam · Hamidreza Bakhshi · Gholamreza Dadashzadeh

Published online: 26 February 2011

Abstract The interference reduction capability of antenna arrays, base station assignment, and the power control algorithms have been considered separately as means to increase the capacity in wireless communication networks. In this paper, we propose smart step closed-loop power control (SSPC) algorithm and base station assignment method based on minimizing the transmitter power (BSA-MTP) technique for direct sequence-code division multiple access (DS-CDMA) receiver in a 2D urban environment. This receiver consists of conjugate gradient adaptive beamforming and matched filter in two stages using antenna arrays. In addition, we study an analytical approach for the evaluation of the impact of power control error (PCE) on the DS-CDMA cellular systems. The simulation results indicate that the SSPC algorithm and the BSA-MTP technique can significantly improve the network bit error rate in comparison with conventional methods. Our proposed methods can also significantly save total transmit power and extend battery life in mobile units. In addition, we show that the convergence speed of the SSPC algorithm is faster than that of conventional algorithms. Finally, we discuss two parameters of PCE and channel propagation conditions (path-loss parameter and variance of shadowing) and their effects on the capacity of the system via some computer simulations.

Keywords Base station assignment · Closed-loop power control · Conjugate gradient adaptive beamforming · Power control error

M. Dosaranian-Moghadam (✉)
Department of Electrical Engineering, Science and Research Branch, Islamic Azad University, Tehran, Iran
e-mail: m_dmoghadam@qiau.ac.ir

H. Bakhshi · G. Dadashzadeh
Department of Electrical Engineering, University of Shahed, Tehran, Iran
e-mail: bakhshi@shahed.ac.ir

G. Dadashzadeh
e-mail: gdadashzadeh@shahed.ac.ir

1 Introduction

In response to the ever-increasing demand for cellular/personal communication services, systems based on direct-sequence code-division multiple access (DS-CDMA) are currently being deployed all around the world. The advantages of DS-CDMA for cellular applications include, among others, the universal one-cell frequency reuse, inherent multipath diversity, and soft capacity limit. It is well known that in order to fully exploit the potential advantage of CDMA, power control is required to counteract the effects of the near-far problem, slow shadow fading (large-scale fading) and multipath fading (small-scale fading) [1–4]. The optimum power control law proposed by Gejji [5] has been developed as a function of the distance and the direction from the base station (BS) to provide a more accurate power control scheme. There are two basic types of power control mechanisms: closed-loop power control and open-loop power control. In a closed-loop power control, the base station sends a command to a mobile set (MS) to adjust the transmit power of the mobile according to the received signal power at a base station. Also, closed-loop power control is employed to combat fast channel fluctuations due to fading. Closed-loop algorithms can effectively compensate fading variations when the power control updating time is smaller than the correlation time of the channel. However, in an open-loop power control, a mobile set adjusts its transmit power according to its received power in the downlink. As up and down link transmissions are affected by different small-scale fading, the open-loop power control is unable to combat multipath fading and is used when a signaling link between receiver and transmitter is not available (i.e. when sending a connection or transmission request) or when it is not worth to set up one (i.e. short or infrequent data packet transmissions). As a result, open-loop and closed-loop power controlled transmissions coexist in current systems [6–8]. However, when applying power control in practice the performance is restricted by a number of limitations and therefore, perfect power control (PPC) cannot be achieved. Thus, the main purpose of these systems is to maintain power level variations at a low enough level to avoid drastic reductions in system capacity and, therefore, the effect on system performance of imperfections in power control must be considered [9–11].

On the other hand, it is generally acknowledged that a viable approach for increasing the capacity of DS-CDMA cellular systems in the reverse link (uplink) is represented by antenna arrays [12,13]. Literature available on multiple antenna systems for DS-CDMA covers several aspects, such as capacity evaluation, algorithms for array combining, and space-time channel characterization. A key factor to the success of array systems with DS-CDMA is, in particular, the capability of providing good performance even in the presence of moderate near-far effect, i.e., in the presence of less-stringent forms of reverse link power control. Traditionally, base stations use antenna arrays to enhance link performance, but with the rapid advancement of technology, mobile units have recently started to share this advantage. There are two main techniques that are used to exploit transmit antenna arrays. The first one is space-time coding, which provides diversity in fading environments [14]. The second is beamforming, which provides spatially matched transmission or (in multiuser scenarios) mitigates interference [15–18]. The power gain that is achieved by transmit beamforming is proportional to the number of transmit antennas. The goal of adaptive beamformers is to enhance the desired signal and suppress noise as well as strong interferences at the sensor array output simultaneously. In past years, some interesting approaches for adaptive beamforming have been suggested to provide robustness against various mismatches in the channel state information for line of sight (LoS) propagation environments, e.g., [18–20]. In addition, the problem of robust beamforming for flat fading channels was considered in [15]. Also, in [21], it is proposed a new beamforming scheme which can transmit multiple data streams

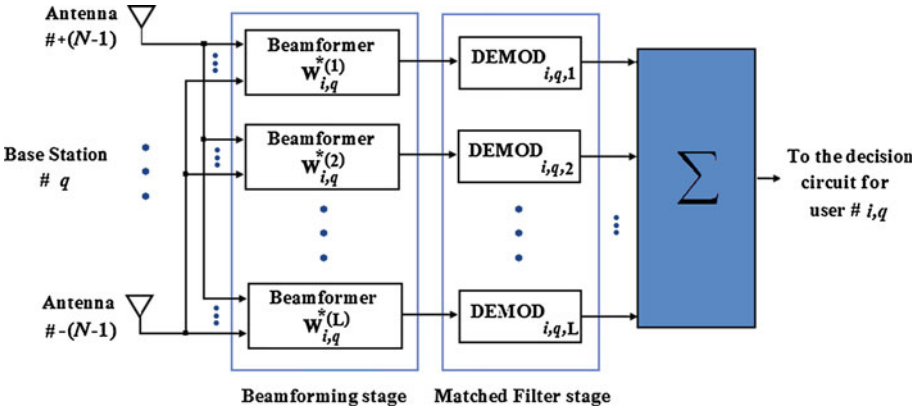

Fig. 1 Block diagram of a two-stage RAKE receiver in DS-CDMA system [27]

simultaneously in multiple-input multiple-output (MIMO) channels by generalizing transmit maximal ratio combining technique. Recently, the robustness of transmit beamforming from the worst-case robustness perspective is studied in [16]. In this paper, we use three adaptive beamforming methods for DS-CDMA systems in 2D urban environments for reverse link. For this purpose and in order to realize a 2D urban environment, urban signal propagation simulator (USPS) is designed. This software is implemented for both forward link and reverse link. The performance of the USPS is described in Sect. 2.

The first contribution of this paper is to extend results previously obtained by the authors in [22–26] for joint multiple-cell system, adaptive beamforming, closed-loop power control, and power control error (PCE) in a 2D urban environment. Accordingly, in this paper we present smart step closed-loop power control (SSPC) algorithm for DS-CDMA cellular systems in a 2D urban environment. This algorithm is a variable and smart step algorithm based on signal to interference plus noise ratio (SINR) measurement in base station. This algorithm can significantly save total transmit power (TTP) and extends the battery life in mobile units. The other advantages of the SSPC algorithm are its simplicity and fast convergence, which make it a practical algorithm in wireless systems. In this paper, we also consider the effect of PCE on DS-CDMA cellular systems in a 2D urban environment.

In this paper, a RAKE receiver in DS-CDMA system is analyzed in two stages according to Fig. 1 [27,28]. In the first stage, this receiver uses conjugate gradient (CG) adaptive beamforming to find optimum antenna weights assuming perfect estimation of the channel parameters (direction, delay, and power) for the desired user. The desired user resolvable directions are fed to the CG beamformer to cancel out the inter-path interference (IPI) from other directions. Also, the RAKE receiver uses conventional demodulation in the second stage to reduce multiple-access interference (MAI). Reducing the MAI will further decrease the system BER. Finally, the output signals from the matched filters (MFs) are combined and then are fed into the decision circuit of the desired user. In this paper, we also use constrained least mean squared (CLMS) algorithm and the switched-beam (SB) technique in the first stage of the RAKE receiver.

On the other hand, the second contribution of this paper is to use a base station assignment technique in urban environments. In [29], the authors combined the base station assignment and power control to increase the reverse link capacity in cellular communication networks. In that work, it was shown that if there exists at least one feasible base station assignment, the

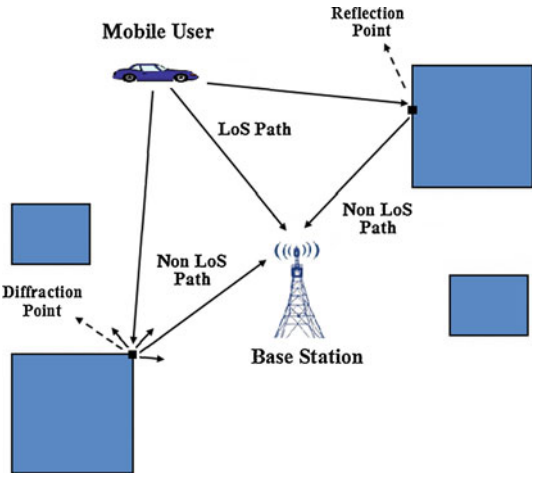

Fig. 2 Diffraction phenomena and reflection phenomena in the USPS software (LoS and Non-LoS paths) for a 2D urban environment in reverse link

proposed algorithm will find the jointly optimal base station assignment and minimal transmitter power level for all users. In this paper, we present base station assignment method based on minimizing the transmitter power (BSA-MTP) technique for achieving target BER in all cells in a 2D urban environment [30].

The organization of the remainder of this paper is as follows. The system model is presented in Sect. 2. The RAKE receiver structure is described in Sect. 3. In Sect. 4, we propose the SSPC algorithm. Then in Sect. 5, we extend the analysis to the case of PCE on DS-CDMA cellular systems in a 2D urban environment. In Sect. 6, the BSA-MTP technique is presented. Section 7 describes the CLMS algorithm and the SB technique. Finally, simulation results and conclusions are given in Sects. 8 and 9, respectively.

2 System Model

2.1 Propagation Model in 2D Urban Environment

Because of using 2D urban structure in this paper, for computing yield for the path between a mobile set and base station (reverse link), propagation model is dramatized in urban environments. Accordingly, with USPS software, mobile set antenna radiate beams which diffuse in all directions and parts of the beams reach to base station. In this software, delivered beam from mobile set by the time of collision to an obstacle like a wall surface or a building, reflects to a new angle and continues its path, which is called reflection phenomena. In condition that radiated beam is conflicted to an obstacle edge, then diffraction phenomena is happened and diffracting point is diffusing new beams to all directions like a transmitter. All reflected beams will stay in the environment as long as their power is not reduced to a threshold limit. Figure 2 shows both phenomena for LoS and non-LoS paths in reverse link. On the other hand, in this software, the channel is modeled with lognormal distributed shadowing. Accordingly, every pixel of the environment stores all environmental information like receiving power and angle for each path [31–33].

According to the above dramatization, we could see that because of LoS in un-urban environment, only one signal is delivered from each user to a receiver, while in function and because of the elimination phenomena in urban environments, beside to signals which are

delivered to line sight, signals which have difference in phase or domain with this signal are also received by the receiver.

2.2 Channel Model

In this paper, we focus on the uplink communication paths in a DS-CDMA cellular system in a 2D urban environment according to the previous subsection. Initially, we consider L_k paths for each link for user k that is optimally combined through a RAKE receiver according to Fig. 1, where for simplicity we assume $L = \min_k(L_k)$ for all users. Also, we assume that there are M active base stations in the network, with K_m users connected to mth base station. At each base station, an antenna array of S sensors and N weights is employed, where $S = 2N - 1$, to receive signals from all users. Note that in CG adaptation algorithm, unlike other adaptation algorithms, the number of weights is less than the number of sensors. Also, for simplicity we assume a synchronous DS-CDMA scheme and BPSK modulation in order to simplify the analysis of the proposed techniques. Additionally, in this paper we assume a slow fading channel (the channel random parameters do not change significantly during the bit interval). Hence, the received signal in the base station q and sensor s from all users can be written as [22,27,33–35].

$$r_{q,s}(t) = \sum_{k} \sqrt{p'_{k,m}\Gamma_k(x,y)} \sum_{l=1}^{L} \sqrt{\alpha_{k,m,l}}\, b_{k,m}\left(t - \tau_{k,m,l}\right) c_{k,m}\left(t - \tau_{k,m,l}\right) \times \exp\left(-j2\pi s d \sin\theta_{k,m,l}/\lambda\right) + n(t) \tag{1}$$

where $c_{k,m}(t)$ is the pseudo noise (PN) chips of user k in cell m (user k, m) with a chip period of T_c; $b_{k,m}(t)$ is the information bit sequence of user k, m with a bit period of $T_b = GT_c$ where G is processing gain; $\tau_{k,m,l}$ is the lth path time delay for user k, m; $\theta_{k,m,l}$ is the direction of arrival (DoA) in the lth path for user k, m; λ is signal wavelength; d is the distance between the antenna elements that in order to avoid the spatial aliasing should be defined as $d = 0.5\lambda$; $n(t)$ is an additive white Gaussian noise (AWGN) process with a two-sided power spectral density (PSD) of $N_0/2$. Also $\Gamma_k(x, y)$ in conventional BSA is defined as

$$\Gamma_k(x,y) = \begin{cases} 1 & ; k \in S_{\mathrm{BS}q} \\ \dfrac{\min\limits_{m\in\Theta_k}\{1/G_{k,m}\}}{1/G_{k,q}} & ; k \in S_o \end{cases} \tag{2}$$

where $G_{k,m}$ and $G_{k,q}$ are the best link gain between user k and BS m and BS q, respectively. It should be mentioned that in USPS, the channel is modeled as a lognormal distributed shadowing with mean 0 and variance σ_ξ^2, thus, the link gains are the function of σ_ξ^2. Also the variable Θ_k defines the set of the nearest BSs to user k and $S_{\mathrm{BS}q}$ is the set of users that connected to BS q and S_o is the set of users that not connected to BS q [6]. Also in (1), $\alpha_{k,m,l}$ is the normalized attenuation in USPS by the best link gain ($G_{k,m}$) between user k and BS m in the lth path, therefore $0 < \alpha_{k,m,l} \leq 1$. Also in (1),

$$p'_{k,m} = G_{k,m} p_{k,m} \tag{3}$$

is the received power in the BS m of user k, m in the presence of closed-loop power control, where $p_{k,m}$ is the transmitted power of user k, m. It is worth mentioning that in the case of PPC, $p'_{k,m}$ is fixed for all users within cell m (i.e., $p'_{k,m} = P = E_b/T_b$, where E_b is the energy per bit for all users).

Accordingly, the received signal in the base station q in sensor s for user i, q is given by [22,27]

$$r'_{i,q,s}(t) = \sum_{l=1}^{L} \sqrt{p'_{i,q}\alpha_{i,q,l}} b_{i,q}\left(t-\tau_{i,q,l}\right) c_{i,q}\left(t-\tau_{i,q,l}\right) \exp\left(-j2\pi sd\sin\theta_{i,q,l}/\lambda\right) + I_{i,q,s}(t) + n(t) \tag{4}$$

where $I_{i,q,s}(t)$ is the interference for user i, q in sensor s and can be shown to be

$$I_{i,q,s}(t) = \sum_{m=1}^{M} \sum_{\substack{k=1 \\ k,m\neq i,q}}^{K_m} \sum_{l=1}^{L} \sqrt{p'_{k,m}\alpha_{k,m,l}\Gamma_k(x,y)} b_{k,m}\left(t-\tau_{k,m,l}\right) c_{k,m}\left(t-\tau_{k,m,l}\right) \times \exp\left(-j2\pi sd\sin\theta_{k,m,l}/\lambda\right) \tag{5}$$

where K_m is the number of users in cell m and M is the number of base stations/cells.

3 Rake Receiver Performance Analysis

The RAKE receiver structure in the DS-CDMA system is shown in Fig. 1. The received signal is spatially processed by a beamforming circuit with the CG adaptive beamforming (CGBF) algorithm, one for each resolvable path (L beamformers). The resultant signal is then passed on to a set of parallel matched filters, on a finger-by-finger basis. Also, the output signals from the L matched filters are combined and then fed into the decision circuit for the desired user.

3.1 Conjugate Gradient Adaptive Beamforming

It is well known that an array of N weights has $N-1$ degree of freedom for adaptive beamforming. This means that with an array of N weights, one can generate $N-1$ pattern nulls and a beam maximum in desired directions. From (5), it is clear that the number of users is $K_u = \sum_{m=1}^{M} K_m$ and the number of interference signals is $LK_u - 1$. To nullify all of these interference signals, one would have to have LK_u weights, which is not practical. So, we focus only on the L paths of the desired user (inter-path interference). Thus, the minimum number of the antenna array weights is L where, typically, L varies from 2 to 6 [34,35].

In this paper, we use the CGBF algorithm that is used based on orthogonal principle [27,28]. On this basis, a set of vectors $\mathbf{w}_i$ is to be selected such that they are $\mathbf{A}$-orthogonal, i.e., $\langle \mathbf{A}\mathbf{w}_i, \mathbf{A}\mathbf{w}_j \rangle = 0$ for $i \neq j$. The optimum weights at time n are obtained by minimizing [27]

$$\left\| \mathbf{x}_{i,q}^{(j)}(n) \right\|^2 = \mathbf{x}_{i,q}^{H(j)}(n)\mathbf{x}_{i,q}^{(j)}(n) \tag{6}$$

where

$$\mathbf{x}_{i,q}^{(j)}(n) = \mathbf{A}_q \mathbf{w}_{i,q}^{(j)}(n) - \mathbf{y}_{i,q}^{(j)} \tag{7}$$

and using (1),

$$\mathbf{A}_q = \begin{bmatrix} r_{q,-(N-1)} & \cdots & r_{q,0} \\ \cdot & \cdot & \cdot \\ r_{q,0} & \cdots & r_{q,+(N-1)} \end{bmatrix} \tag{8}$$

is the $N \times N$ signal matrix in the base station q. Also,

$$\mathbf{y}_{i,q}^{(j)} = \left[e^{-j(N-1)\theta_{i,q,j}/2} \ldots 1 \ldots e^{+j(N-1)\theta_{i,q,j}/2} \right]^T \tag{9}$$

and

$$\mathbf{w}_{i,q}^{(j)}(n) = \left[w_{i,q,0}^{(j)}(n) w_{i,q,1}^{(j)}(n) \ \ldots \ w_{i,q,N-1}^{(j)}(n) \right]^T \tag{10}$$

are the excitation and weight vectors ($N \times 1$) for user i, q in the jth path, respectively.

It should be mentioned that the CG algorithm has two main characteristics [27]:

1. This algorithm can produce a solution of the matrix equation very efficiently and converge in a finite number of iterations (the number of beamformer weights).
2. Convergence is guaranteed for any possible condition of the signal matrix, according to (8).

According to the algorithm of CG, the updated value of the weight vector for user i, q in the jth path at time $n+1$ is computed by using the simple recursive relation [27,28]:

$$\mathbf{w}_{i,q}^{(j)}(n+1) = \mathbf{w}_{i,q}^{(j)}(n) + \kappa_{i,q}^{(j)}(n) \boldsymbol{\beta}_{i,q}^{(j)}(n) \tag{11}$$

where

$$\begin{aligned}
\kappa_{i,q}^{(j)}(n) &= \left\| \mathbf{A}_q^H \mathbf{x}_{i,q}^{(j)}(n) \right\|^2 \Big/ \left\| \mathbf{A}_q \boldsymbol{\beta}_{i,q}^{(j)}(n) \right\|^2 \\
\mathbf{x}_{i,q}^{(j)}(n+1) &= \mathbf{x}_{i,q}^{(j)}(n) + \kappa_{i,q}^{(j)}(n) \boldsymbol{\beta}_{i,q}^{(j)}(n) \\
\boldsymbol{\beta}_{i,q}^{(j)}(0) &= -\mathbf{A}_q^H \mathbf{x}_{i,q}^{(j)}(0) \\
\boldsymbol{\beta}_{i,q}^{(j)}(n+1) &= \mathbf{A}_q^H \mathbf{x}_{i,q}^{(j)}(n+1) + \eta_{i,q}^{(j)}(n) \boldsymbol{\beta}_{i,q}^{(j)}(n) \\
\eta_{i,q}^{(j)}(n) &= \left\| \mathbf{A}_q^H \mathbf{x}_{i,q}^{(j)}(n+1) \right\|^2 \Big/ \left\| \mathbf{A}_q^H \mathbf{x}_{i,q}^{(j)}(n) \right\|^2
\end{aligned} \tag{12}$$

The output signal from the jth CG beamformer ($j = 1, \ldots, L$) can be written as

$$y_{i,q}^{(j)}(t) = \sqrt{p'_{i,q} \alpha_{i,q,j}} b_{i,q}\left(t - \tau_{i,q,j}\right) c_{i,q}\left(t - \tau_{i,q,j}\right) + I_{i,q}^{(j)}(t) + n^{(j)}(t) \tag{13}$$

where $n^{(j)}(t)$ is a zero mean Gaussian noise of variance σ_n^2 and $I_{i,q}^{(j)}(t)$, the MAI, is defined as

$$\begin{aligned}
I_{i,q}^{(j)}(t) = \sum_{m=1}^{M} \sum_{\substack{k=1 \\ k,m \neq i,q}}^{K_m} \sum_{l=1}^{L} \sqrt{p'_{k,m} \alpha_{k,m,l} \Gamma_k(x,y)} g_{i,q}^{(j)}\left(\theta_{k,m,l}\right) b_{k,m}(t - \tau_{k,m,l}) \\
\times c_{k,m}\left(t - \tau_{k,m,l}\right)
\end{aligned} \tag{14}$$

where

$$g_{i,q}^{(j)}(\theta) = \left[e^{-j(N-1)\theta/2} \ldots 1 \ldots e^{+j(N-1)\theta/2} \right] \times \mathbf{w}_{i,q}^{(j)} \tag{15}$$

is the magnitude response of the jth beamformer for user i, q toward the direction of arrival θ and $\mathbf{w}_{i,q}^{(j)}$ is the jth beamformer's weight vector for user i, q.

3.2 Matched Filter Stage

Using beamforming will only cancel out the IPI for the desired user and will reduce the MAI from the users whose signals arrive at different angles from the desired user signal (out-beam interference). Now, in the second stage of the RAKE receiver, the output signal from the jth beamformer directly passes on to a filter matched to the desired user's signature sequence. The jth matched filter output corresponding to the nth bit is [22,27]:

$$z_{i,q}^{(j)}(n) = \sqrt{p'_{i,q}\alpha_{i,q,j}}\, b_{i,q}(n) + I'^{(j)}_{i,q}(n) + n'^{(j)}(n) \tag{16}$$

where

$$I'^{(j)}_{i,q}(n) = \frac{1}{T_b} \int_{(n-1)T_b+\tau_{i,q,j}}^{nT_b+\tau_{i,q,j}} I_{i,q}^{(j)}(t) c_{i,q}\left(t-\tau_{i,q,j}\right) dt \tag{17}$$

and

$$n'^{(j)}(n) = \frac{1}{T_b} \int_{(n-1)T_b+\tau_{i,q,j}}^{nT_b+\tau_{i,q,j}} n^{(j)}(t) c_{i,q}\left(t-\tau_{i,q,j}\right) dt \tag{18}$$

If we assume that the paths' delays from all users are less than the symbol duration $\left(\tau_{k,m,l} < T_b\right)$ for all users' signals on all paths, the nth bit MAI at the output of the jth matched filter is expressed as

$$\begin{aligned} I'^{(j)}_{i,q}(n) = \sum_{m=1}^{M} \sum_{\substack{k=1 \\ k,m\neq i,q}}^{K_m} \sum_{l=1}^{L} \sqrt{p'_{k,m}\alpha_{k,m,l}\Gamma_k(x,y)}\, g_{i,q}^{(j)}\left(\theta_{k,m,l}\right) b_{k,m}(n) \\ \times R_{i,k}(\tau_{i,q,j} - \tau_{k,m,l}) \end{aligned} \tag{19}$$

where the autocorrelation function $R_{i,k}(\tau)$ is [36]:

$$R_{i,k}(\tau) = \frac{1}{T_b} \int_{T_b} c_{i,q}(t)\, c_{k,m}(t+\tau)\, dt \tag{20}$$

If all users' delays are multiples of the chip period (T_c), then

$$R_{i,k}(\tau) = \frac{1}{G} \sum_{l_1=0}^{G-1} \sum_{l_2=0}^{G-1} c_{i,q}(l_1)\, c_{k,m}(l_2) R_c(\tau - (l_1 - l_2)\, T_c) \tag{21}$$

where the autocorrelation function $R_c(\tau)$ is:

$$R_c(\tau) = \frac{1}{T_b} \int_{T_b} c(t)\, c(t+\tau)\, dt \tag{22}$$

In the case of a maximal-length sequence (m-sequence) and for $0 \le \tau \le T_b$, we have [36]:

$$R_c(\tau) = \begin{cases} 1 - \frac{|\tau|}{T_c}(1 + 1/G) & ; |\tau| \le T_c \\ -1/G & ; |\tau| \ge T_c \end{cases} \tag{23}$$

Now, the SINR in output of the RAKE receiver for user i, q is given as [27,37]

$$\mathrm{SINR}_{i,q}(\alpha) = \sum_{j=1}^{L} \mathrm{SINR}_{i,q}^{(j)}(\alpha) \tag{24}$$

where

$$\mathrm{SINR}_{i,q}^{(j)}(\alpha) = \frac{p'_{i,q}\alpha_{i,q,j}}{\mathrm{E}\left(I'^{(j)}_{i,q}\right)^2 + \mathrm{E}\left(n'^{(j)}\right)^2} \tag{25}$$

is the SINR in output of the RAKE receiver in path j for user i, q and $\mathrm{E}(.)$ is denoted the expectation.

Now, we can rewrite the SINR in (25) as follows.

$$\mathrm{SINR}_{i,q}^{(j)}(\alpha) = \frac{p'_{i,q}\alpha_{i,q,j}}{\sum_{m=1}^{M}\sum_{k=1;k,m\neq i,q}^{K_m} p'_{k,m}\Gamma_k(x,y)\sum_{l=1}^{L}\alpha_{k,m,l}\left|g_{i,q}^{(j)}\left(\theta_{k,m,l}\right)\right|^2 R_{i,k}^2\left(\tau_{i,q,j}-\tau_{k,m,l}\right)+\frac{N_0}{2T_b}} \tag{26}$$

In order to perform the BER, we assume Gaussian approximation for the probability density function of interference plus noise. The conditional BER for a BPSK modulation is [27,36]:

$$\mathrm{BER}_{i,q}(\alpha) = Q\left(\sqrt{2\times \mathrm{SINR}_{i,q}(\alpha)}\right) \tag{27}$$

where

$$Q(x) = \frac{1}{\sqrt{2\pi}}\int_{x}^{\infty}\exp\left(-u^2/2\right)du \tag{28}$$

4 Smart Step Closed-Loop Power Control Algorithm

A major limiting factor for the satisfactory performance of CDMA systems is the near-far effect. Power control is an intelligent way of adjusting the transmitted powers in cellular systems so that the TTP is minimized, but at the same time, the user SINRs satisfies the system quality of service (QoS) requirements [38,39].

Depending on the execution location, power control algorithms can be categorized as either centralized and distributed [1–9,34,40]. In centralized power control, a network center can simultaneously compute the optimal power levels for all users. However, it requires measurement of all the link gains and the communication overhead between a network center and base stations. Thus, it is difficult to realize in a large system [41]. Distributed power control, on the other hand, uses only local information to determine transmitter power levels. It is much more scalable than centralized power control. However, transmitter power levels may not be optimal, resulting in performance degradation [42].

The distributed closed-loop power control problem has been investigated by many researchers from many perspectives during recent years [8,38,42]. For instance, the conventional fast closed-loop power control strategy used in practice in CDMA systems is a

fixed step controller based on SINR measurements. The fixed step closed-loop power control (FSPC) algorithm is defined by [8]

$$p_{i,q}^{n'+1} = p_{i,q}^{n'} + \delta \text{sign}\left(\gamma_{i,q}^{*} - \gamma_{i,q}^{n'}\right) \tag{29}$$

where $p_{i,q}^{n'}$, $\gamma_{i,q}^{*}$, and $\gamma_{i,q}^{n'}$ are the transmitter power, SINR target, and measured SINR of user i, q at time n', respectively, and δ is the fixed step size. Also $p_{i,q}^{n'+1}$ is transmitter power control (TPC) command in the feedback link of the base station to user i, q at time $n' + 1$(all signals are in decibels).

Also, the distributed traditional closed-loop power control (DTPC) is defined by [38]

$$p_{i,q}^{n'+1} = \frac{\gamma_{i,q}^{*}}{\gamma_{i,q}^{n'}} p_{i,q}^{n'} \tag{30}$$

In both algorithms, the simple intuition behind this iteration is that if the current SINR $\gamma_{i,q}^{n'}$ of user i, q is less than the target SINR $\gamma_{i,q}^{*}$, then the power of that user is increased; otherwise, it is decreased.

It should be mentioned that convergence speed of DTPC algorithm is higher than that of FSPC algorithm. Also, the variance of the SINR mis-adjustment in FSPC algorithm is higher than that of DTPC algorithm. But it has been shown that the FSPC algorithm converges to $\left|\gamma_{i,q}^{*} - \gamma_{i,q}^{n'}\right| \leq 2\delta k_d$, where k_d is the loop delay [7].

Also in [43], variable step closed-loop power control (VSPC) algorithm has been proposed. In this algorithm, variable step size is discrete with mode q_v. It is shown that the performance of VSPC algorithm with mode $q_v = 4$ is found to be worse than that of a fixed step algorithm ($q_v = 1$) under practical situations with loop delay of two power control intervals, but the convergence speed of VSPC algorithm is higher than that of FSPC algorithm. Also in this algorithm, the variance of the SINR mis-adjustment is reduced when compared to the FSPC algorithm.

Practical implementations of power control in CDMA systems utilize closed-loop control, where the transmitter adjusts its power based on commands received from the receiver in a feedback channel. To minimize signaling overhead, typically one bit is used for the power control command. In practice, the command must be derived based on measurements made at the receiver, transmitted over the feedback channel to the transmitter, and finally processed and applied at the transmitter. All these operations constitute a loop delay, which can cause problems if it is not properly taken care of in the design of the power control algorithm. In many cases the loop delay is known due to a specific frame structure inherent in the system. A typical loop delay situation encountered in wideband CDMA (WCDMA) systems is shown in Fig. 3. The slot at time $n't$ is transmitted using power $p^{n'}$. The receiver measures the SINR $\gamma^{n'}$ over a number of pilot and/or data symbols and derives a TPC command. The command is transmitted to the transmitter in the feedback link and the transmitter adjusts its power at time $\left(n' + 1\right) t$ according to the command. It should be mentioned that since the power control signaling is standardized, the loop delays are known exactly [8].

In this paper, we propose the smart step closed-loop power control algorithm. We express the SSPC algorithm as follows.

$$p_{i,q}^{n'+1} = p_{i,q}^{n'} + \delta \left|\gamma_{i,q}^{*} - \gamma_{i,q}^{n'}\right| \text{sign}\left(\gamma_{i,q}^{*} - \gamma_{i,q}^{n'}\right) \tag{31}$$

Performance of the SSPC algorithm is shown in Fig. 4. This algorithm is implemented as follows.

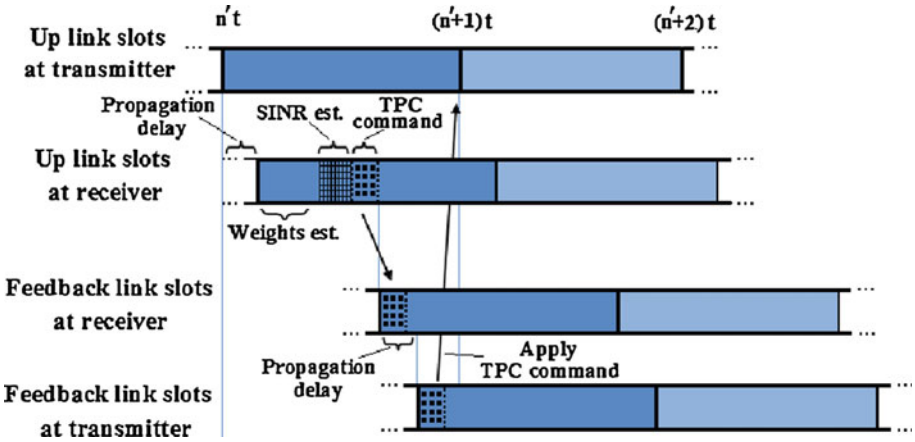

Fig. 3 Example of power control timing in WCDMA systems [8]

1. Select the initial transmitted power vector ($n' = 0$) for all users within cell m as

$$\mathbf{p}_m^0 = \left[p_{1,m}^0 p_{2,m}^0 \cdots p_{K_m,m}^0\right], \quad m = 1, 2, \ldots, M$$

2. Estimate the weight vector for all users with the CGBF algorithm using (11).
3. Calculate the SINR for all users using (24).
4. If $\left|\gamma_{k,m}^* - \gamma_{k,m}^{n'}\right| > \varepsilon_0$ for each user then set $n' = n' + 1$ and calculate the TPC for all users at time $n' + 1$ using (31) and go back to step 2., where ε_0 is the threshold value.
5. Finally, if $\left|\gamma_{k,m}^* - \gamma_{k,m}^{n'}\right| < \varepsilon_0$ for all users then algorithm ends.

As will be seen from simulation results, because of variable coefficient in the sign function, the convergence speed of our algorithm is higher than that of FSPC and VSPC algorithms.

5 Power Control Error

When imperfections in power control are considered, multipath fading is not perfectly compensated. As a result, the power received from a mobile will not be constant at the base station to which the mobile is connected. Accordingly, we can rewrite (1) as follows [11,27]

$$r_{q,s}(t) = \sum_k \sqrt{P\lambda_{k,m}\Gamma_k(x,y)} \sum_{l=1}^{L} \sqrt{\alpha_{k,m,l}} b_{k,m}\left(t - \tau_{k,m,l}\right) c_{k,m}\left(t - \tau_{k,m,l}\right) \times \exp\left(-jsk_d \sin\theta_{k,m,l}\right) + n(t) \tag{32}$$

where $P = E_b/T_b$ represents the received signal power of all users within cell q in the presence of PCE. The variable $\lambda_{k,m}$ is PCE for user k, m, which is assumed to follow a log-normal distribution and thus can be written as $\lambda_{k,m} = 10^{\upsilon_{k,m}/10}$, where $\upsilon_{k,m}$ is a Gaussian random variable with mean 0 and variance σ_υ^2 for all users [6]. On the other hand, $\mathrm{E}\left[\lambda_{k,m}\right]$ for all users can be written as follows [11]

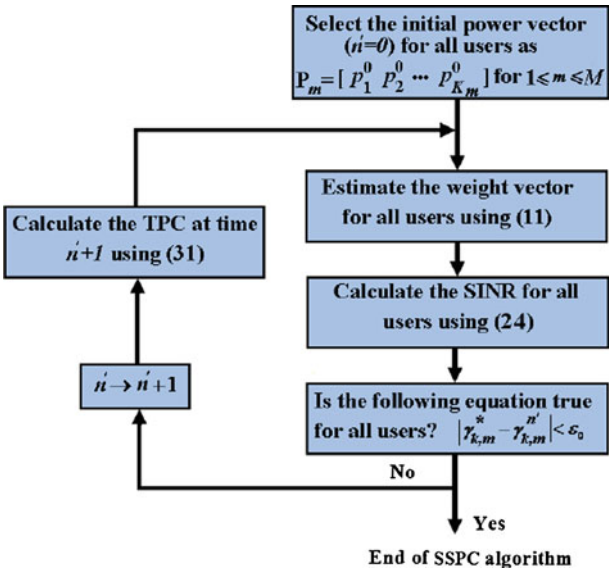

Fig. 4 Block diagram for SSPC algorithm

$$\mathrm{E}\left[\lambda_{k,m}\right] = e^{\beta^2\sigma_\upsilon^2/2} \tag{33}$$

where $\beta = \ln(10)/10$. Accordingly, we can rewrite the SINR in (25) as follows.

$$\mathrm{SINR}_{i,q}^{(j)}(\alpha) = \frac{P e^{\beta\upsilon_{i,q}}\alpha_{i,q,j}}{\mathrm{E}\left(I_{i,q}^{\prime(j)}\right)^2 + \mathrm{E}\left(n^{\prime(j)}\right)^2} \tag{34}$$

Using (26) and (33), we can rewrite the SINR in (34) as follows [11,44].

$$\mathrm{SINR}_{i,q}^{(j)}(\alpha) = \frac{e^{\beta\upsilon_{i,q}}\alpha_{i,q,j}}{e^{\beta^2\sigma_\upsilon^2/2}\sum_{m=1}^{M}\sum_{k=1;k,m\neq i,q}^{K_m}\Gamma_k(x,y)\sum_{l=1}^{L}\alpha_{k,m,l}\left|g_{i,q}^{(j)}\left(\theta_{k,m,l}\right)\right|^2 R_{i,k}^2\left(\tau_{i,q,j}-\tau_{k,m,l}\right)+\frac{0.5}{E_b/N_0}} \tag{35}$$

6 The BSA-MTP Technique

To improve the performance of cellular systems, base station assignment technique can be used. In the joint power control and base station assignment, a number of base stations are potential receivers of a mobile transmitter. Accordingly, the objective is to determine the assignment of users to base stations which minimizes the allocated mobile powers. In simple mode and in multiple-cell systems, the user is connected to the nearest base station. This method is not optimal in cellular systems under the shadowing and multipath fading channels and can increase the system BER [29,45].

The system capacity might be improved if the users are allowed to switch to alternative base stations, especially when there are congested areas in the network. Obviously, when uplink

performance is of concern, the switching should happen based on the total interferences seen by the base stations [45].

So far, we have considered the power control problem for a number of transmitter-receiver pairs with fixed assignments, which can be used in uplink or downlink in mobile communication systems. In an uplink scenario where base stations are equipped with antenna arrays, the problem of joint power control and beamforming, as well as base station assignment, naturally arises. In this paper, we modify the BSA-MTP technique to support base station assignment as well in a 2D urban environment. The modified technique can be summarized as follows.

1. Initially by the conventional BSA technique, each mobile connects to its base station, according to (2).
2. Estimate the weight vector for all users with the CGBF algorithm using (11).
3. Calculate the transmitted power of all users using (3).
4. Finally, $K_r = \lfloor K_u/(M+1) \rfloor$ users whose transmitted power is higher than that of the other users are transferred to other base stations according to the following equation, where the function $\lfloor x \rfloor$ returns the integer portion of a number x.

$$\Gamma_k(x, y) = \begin{cases} 1 & ; \quad k \in S_{\mathrm{BS}q} \\ \dfrac{\min\limits_{m \in \Theta_k} \{1/G_{k,m}\}}{1/G_{k,q}} & ; \quad k \in S_{\overline{\mathrm{BS}q}} \\ \dfrac{\min\limits_{m \in \Theta_k} \{1/G_{k,m}\}}{1/G_{k,q}} & ; \quad k \in S_o \end{cases} \tag{36}$$

where $S_{\overline{\mathrm{BS}q}}$ is the set of users that are in cell q but not connected to BS q [4].

It should be mentioned that the use of the technique for users that are present on the border of cells, the BER can be effectively reduced.

7 Other Beamforming Methods

7.1 Constrained LMS Algorithm

Constrained LMS algorithm is a gradient based algorithm to minimize the total processor output power, based on the look direction constraint. The adaptive algorithm is designed to adapt efficiently to the environment and is able to permanently preserve the desired frequency response in the look direction while minimizing the output power of the array. In [22,26], we used the CLMS algorithm in order to decrease the interference of DS-CDMA cellular systems in multipath fading channels. In this algorithm, unlike the CGBF algorithm, the number of weights and sensors are equal, i.e., $S = N$. Accordingly, by the CLMS algorithm, desired users' signal in an arbitrary path is passed but the IPI is not canceled in other paths in each RAKE finger, while the IPI is removed in the CGBF algorithm.

Accordingly, the output of the array with the CLMS algorithm in the nth iteration in the jth path for user i, q is given by [22,44,46]

$$y_{i,q}^{(j)}(n) = \mathbf{w}_{i,q}^{(j)}(n)^H \mathbf{r}'_{i,q}(n) \tag{37}$$

where $\mathbf{r}'_{i,q} = \left[r'_{i,q,0} r'_{i,q,1} \cdots r'_{i,q,N-1} \right]^T$.

The expected output power of the array in the nth iteration is given by

$$\begin{aligned} \mathrm{E}\left(\left|y_{i,q}^{(j)}(n)\right|^2\right) &= \mathrm{E}\left(y_{i,q}^{(j)}(n) y_{i,q}^{(j)}(n)^*\right) \\ &= \mathrm{E}\left(\mathbf{w}_{i,q}^{(j)}(n)^H \mathbf{r}'_{i,q}(n) \mathbf{r}'_{i,q}(n)^H \mathbf{w}_{i,q}^{(j)}(n)\right) \\ &= \mathbf{w}_{i,q}^{(j)}(n)^H \mathbf{R}_{r'r'} \mathbf{w}_{i,q}^{(j)}(n) \end{aligned} \tag{38}$$

where $\mathbf{R}_{r'r'}$ is the correlation matrix of the received vector $\mathbf{r}'_{i,q}(n)$.

A real-time CLMS algorithm for determining the optimal weight vector for user i, q in the jth path is [22,46]:

$$\begin{cases} \mathbf{w}_{i,q}^{(j)}(n+1) = \mathbf{w}_{i,q}^{(j)}(n) + \mu g\left(\mathbf{w}_{i,q}^{(j)}(n)\right) \\ \mathbf{w}_{i,q}^{(j)H} \mathbf{a}_{i,q}^{(j)}\left(\theta_{i,q,j}\right) = 1 \end{cases} \tag{39}$$

where

$$\mathbf{a}_{i,q}^{(j)}\left(\theta_{i,q,j}\right) = [1 \exp\left(-j2\pi d \sin\theta_{i,q,j}/\lambda\right) \ldots . \exp\left(-j2\pi d(N-1)\sin\theta_{i,q,j}/\lambda\right)]^T \tag{40}$$

denotes spatial response of the array for user i, q in the jth path. Also in (39), $\mathbf{w}_{i,q}^{(j)}(n+1)$ is the new weight computed at the $(n+1)$th iteration for user i, q in the jth path. Also, the variable scalar μ denotes a positive scalar (gradient step size) that controls the convergence characteristic of the algorithm, that is, how fast and how close the estimated weights approach the optimal weights, and $g\left(\mathbf{w}_{i,q}^{(j)}(n)\right)$ denotes an unbiased estimate of the gradient of the power surface $(\mathbf{w}_{i,q}^{(j)}(n)^H \mathbf{R}_{r'r'} \mathbf{w}_{i,q}^{(j)}(n)$ which is the expected output power of the array) with respect to $\mathbf{w}_{i,q}^{(j)}(n)$ after the nth iteration. The algorithm is "constrained" because the weight vector satisfies the constraint at each iteration, that is $\mathbf{w}_{i,q}^{(j)H} \mathbf{a}_{i,q}^{(j)}\left(\theta_{i,q,j}\right) = 1$. We rewrite the CLMS algorithm as follows [22,46]

$$\mathbf{w}_{i,q}^{(j)}(n+1) = \boldsymbol{\psi}_{i,q}^{(j)}\left(\mathbf{w}_{i,q}^{(j)}(n) + \mu g\left(\mathbf{w}_{i,q}^{(j)}(n)\right)\right) + \frac{\mathbf{a}_{i,q}^{(j)}\left(\theta_{i,q,j}\right)}{N} \tag{41}$$

where

$$\boldsymbol{\psi}_{i,q}^{(j)} = \mathbf{I} - \frac{\mathbf{a}_{i,q}^{(j)}\left(\theta_{i,q,j}\right) \mathbf{a}_{i,q}^{(j)}\left(\theta_{i,q,j}\right)^H}{N} \tag{42}$$

The gradient of $\mathbf{w}_{i,q}^{(j)}(n)^H \mathbf{R}_{r'r'} \mathbf{w}_{i,q}^{(j)}(n)$ with respect to $\mathbf{w}_{i,q}^{(j)}(n)$ is given by [46]

$$g\left(\mathbf{w}_{i,q}^{(j)}(n)\right) \triangleq -\frac{\partial}{\partial \mathbf{w}_{i,q}^{(j)*}}\left(\mathbf{w}_{i,q}^{(j)}(n)^H \mathbf{R}_{r'r'} \mathbf{w}_{i,q}^{(j)}(n)\right) = -2\mathbf{R}_{r'r'} \mathbf{w}_{i,q}^{(j)}(n) \tag{43}$$

and its computation using this expression requires knowledge of $\mathbf{R}_{r'r'}$, which normally is not available in practice. For a standard LMS algorithm, an estimate of the gradient at each iteration is made by replacing $\mathbf{R}_{r'r'}$ by its noise sample $\mathbf{r}'_{i,q}(n+1)\,\mathbf{r}'_{i,q}(n+1)^H$ available at time instant $(n+1)$, leading to

$$g\left(\mathbf{w}_{i,q}^{(j)}(n)\right) = -2\mathbf{r}'_{i,q}(n+1)\, y_{i,q}^{(j)*}(n) \tag{44}$$

The CLMS is a fast convergence algorithm. However, it is drastically sensitive to the mismatch in the direction of arrival. Meanwhile, the weights estimated by the standard algorithm

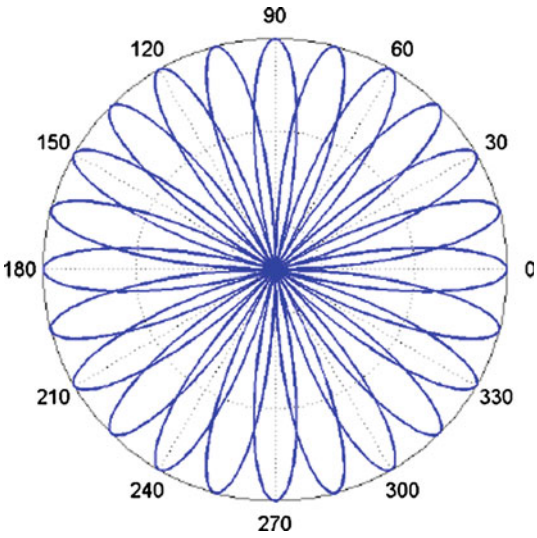

Fig. 5 36 beams in each base station with switched-beam technique

are sensitive to the signal power, requiring a lower step size in the presence of a strong signal for the algorithm to converge, which, in turn, leads to an increase in the convergence time due to a decrease in mis-adjustment error [32,46].

From the above discussion, we can conclude that the BER in the CGBF algorithm is less than that in the CLMS algorithm. In the simulation study, we will evaluate the average BER in a DS-CDMA receiver with the CGBF and CLMS algorithms.

7.2 Switched-Beam Technique

One simple alternative to the fully adaptive antenna is the switched-beam architecture in which the best beam is chosen from a number of fixed steered beams. Switched-beam systems are technologically the simplest and can be implemented by using a number of fixed, independent, or directional antennas [47]. We list the conditions of the SB technique for this paper as follows [31].

1. According to Fig. 5, beams coverage angle is 30° and overlap between consecutive beams is 20°. Thus each base station has 36 beams.
2. According to Fig. 6, each user can use one beam for each of its path to communicate with a base station at any time.

7.3 Equal Sectoring Method

One simple method used to sectorize a cell is equal sectoring; in which all sectors have the same coverage angle. In this paper, we assume three sectors for each base station with sector angle 120° for the ES method [10].

8 Simulation Results

We consider $M = 9$ base stations for a nine-cell DS-CDMA system as Fig. 7. We assume a uniform linear array of S omni-directional antennas in each base station with antenna

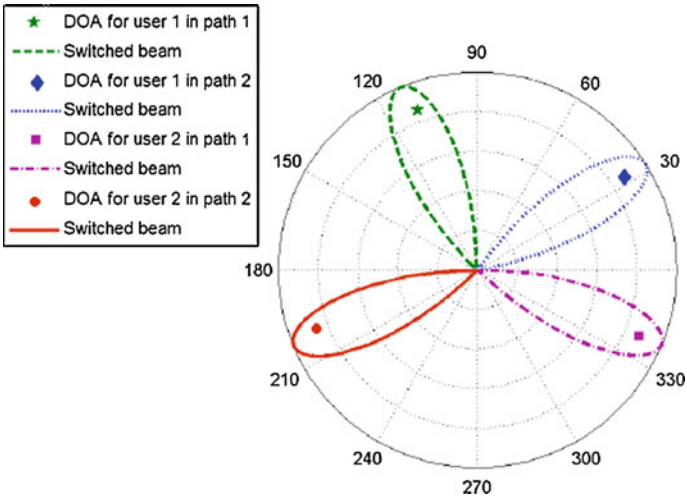

Fig. 6 Select of beam for two users in two paths with switched-beam technique

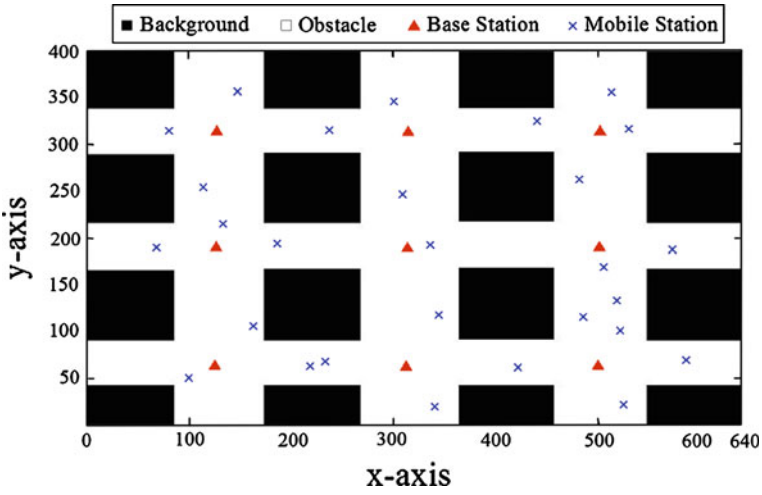

Fig. 7 Placing users and nine base stations in a two-dimensional map

spacing $d = \lambda/2$. Also, we assume the input data rate $T_b = 9.6$ Kbps; the number of antenna weights $N = 3$; the number of antenna sensors in the CGBF algorithm $S = 5$; the number of antenna sensors in the CLMS algorithm $S = 3$; $L = 4$ resolvable propagation paths for all users; resolution, path loss parameter, and variance of the log-normal shadow fading in USPS $R = 1$, $L_p = 0.05$ dB/m, and $\sigma_\xi^2 = 4$ dB, respectively; gradient step size in the CLMS algorithm $\mu = 0.005$; initial value for weight vectors in the CGBF and CLMS algorithms $\mathbf{w}(0) = \mathbf{0}$. The SINR target value is the same for all users and is set to $\gamma^* = 10$ (10 dB). It is also assumed that the distribution of users in all cells is uniform.

In this paper, we use m-sequence generator with processing gain $G = 512$ based on a linear feedback shift register (LFSR) circuit using the Fibonacci feedback approach [36]. This structure is shown in Fig. 8a. Also, according to [36], we use the sequence generated by

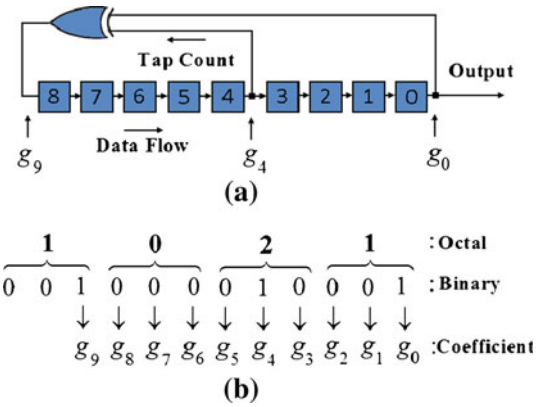

Fig. 8 **a** FiboNacci feedback generator for LFSR polynomial $g(D) = 1 + D^4 + D^9$ for nine-stage shift register. **b** Expanding the octal entry 1021 into binary form [36]

the polynomial corresponding to the entry the octal representation of generator polynomial, ORGP = [1021]* for a nine-stage shift register. Figure 8b shows expanding the octal entry 1021 into binary form. Then, the LFSR polynomial is $g(D) = 1 + D^4 + D^9$.

Figure 9 shows the comparison of the average SINR achieved over $K_u = 120$ users and signal to noise ratio, SNR=10dB, versus the power control iteration index (n') for SSPC, VSPC ($q_v = 4$), and FSPC algorithms and for the BSA-MTP technique (solid line) and conventional BSA technique (dashed line). In this simulation, the two-stage RAKE receiver uses CGBF, CLMS, SB, or ES methods in the first stage. Also, we assume that each user has a maximum power constraint of 1watt. Accordingly, we observe that the convergence speed of the SSPC algorithm is faster than that of the VSPC and FSPC algorithms. For example, the SSPC algorithm with CGBF algorithm converges in about 10 iterations for the BSA-MTP technique, while VSPC and FSPC algorithms converge in about 12 and 17 iterations, respectively. In addition, we see that the convergence speed of the joint SSPC algorithm and the SB technique is faster than that in the other cases. It can also be seen that the convergence speed of the CGBF algorithm is faster than that of the CLMS algorithm. It can be also observed from this figure that the convergence speed with BSA-MTP technique is faster than that with conventional BSA technique. On the other hand, we observe that the average SINR level achieved is below the target SINR value for the ES method, because in this method the MAI is higher than that in CLMS and CGBF algorithms and SB technique.

Figure 10 shows the comparison of TTP usage versus the power control iteration index (n'), as in Fig. 9. But in this simulation, we assume that users no have maximum power constraints. Similar to what we see in Fig. 9, we observe that the ES method can never achieve the target SINR value for all users. Also this figure shows that the SSPC algorithm offers more savings in the TTP as compared with the FSPC and VSPC algorithms. In addition, we can see that the TTP for the joint SSPC algorithm and SB technique is lower than that for the other cases. It can be also observed that the TTP with CLMS algorithm is higher than that with CGBF algorithm and SB technique. For example, with the SSPC algorithm, TTP for the SB technique is 15.5 W for the BSA-MTP technique, while for the CGBF and CLMS algorithms; TTP is 17.15 and 18.95 W, respectively. On the other hand, we observe that the TTP for BSA-MTP technique (solid line) is lower than that for conventional MTP technique (dashed line).

Figure 11 shows the average BER for all users in network versus the SNR for different receivers (one, two-stage receivers), $K_u = 120$ active users, and a log-normally distributed

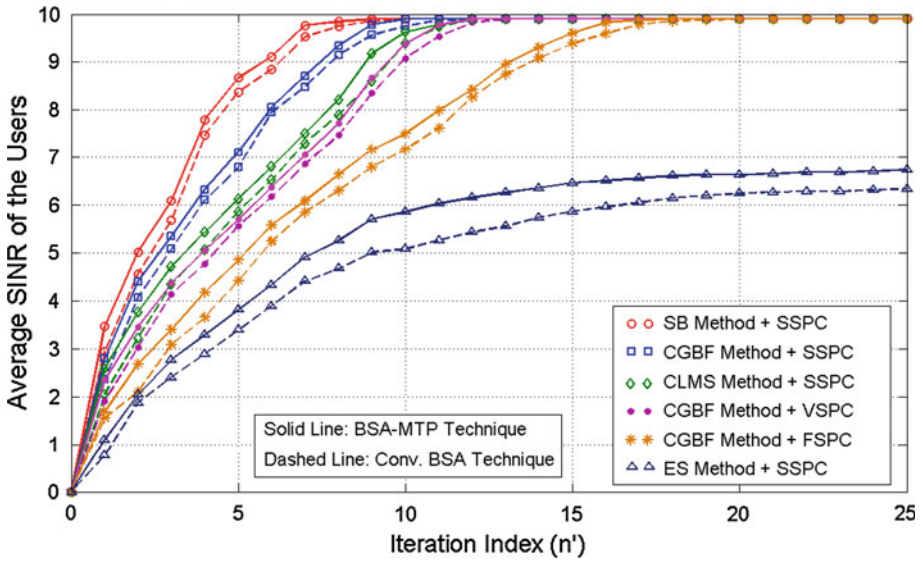

Fig. 9 Average SINR of all users versus power control iteration index (n'), with maximum power constraint of 1 watt, $K_u = 120$, and SNR = 10 dB

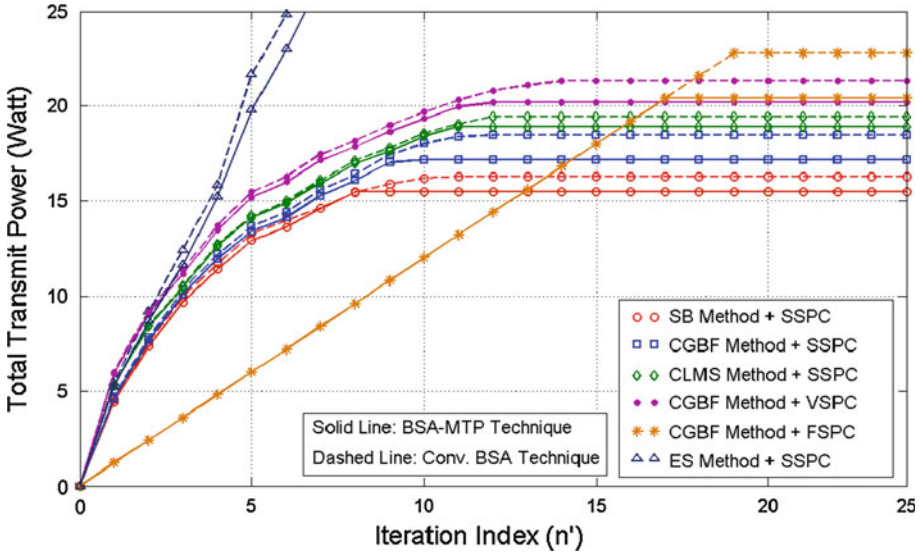

Fig. 10 Total transmit power of all users versus power control iteration index (n'), $K_u = 120$, and SNR = 10 dB. No power constraints

PCE with $\sigma_v^2 = 4$ dB. It should be mentioned that in this simulation, $K_r = 12$ users can be transferred to other base stations with the BSA-MTP technique. It is clear that, in MF only receiver (one-stage receiver) and in the case of the conventional BSA technique, we still have the error floor at high SNR. Also, CGBF and MF receiver (the two-stage RAKE receiver as Fig. 1) have a better performance compared with MF only receiver. In addi-

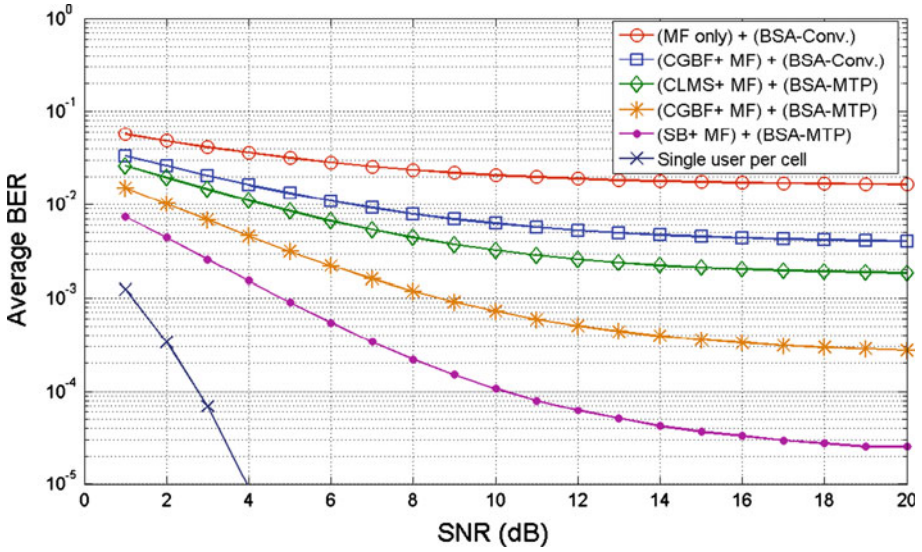

Fig. 11 Average BER versus the SNR for $\sigma_\upsilon^2 = 4$ dB and $K_u = 120$

tion, we observe that using the BSA-MTP technique in CGBF and MF receiver, the average BER is lower than the conventional BSA technique. For example, at a SNR of 10dB, the average BER is 0.0062 for the two-stage RAKE receiver with the conventional BSA technique, while for the BSA-MTP technique, the average BER is 0.0007. Also, it can be seen that the average BER in the CLMS algorithm is higher than that in the CGBF algorithm, because in CGBF algorithm the IPI is removed whereas in CLMS algorithm it is not canceled. Also, we observe that using the BSA-MTP technique in SB and MF receiver, the average BER is lower than that in the other cases. For example, at a SNR of 8 dB, the average BER using the BSA-MTP technique is 0.0002 for SB technique, while the average BER for CGBF and CLMS algorithms is 0.0012 and 0.0044, respectively. Also, it is clear that the MAI is not removed totally and the performance is still worse than the single user per cell bound.

Results for the average BER versus the SNR for CGBF and MF receiver and $K_u = 120$ active users, and different values of σ_υ^2 are provided in Fig. 12. In this figure, similar to what we see in Fig. 11, we observe that the average BER for the BSA-MTP technique is lower than that for the conventional BSA technique. Also, it can be seen that the average BER for $\sigma_\upsilon^2 = 0$ dB (perfect power control) is lower than that for the other cases. For example, at a SNR of 12 dB and for the BSA-MTP technique, the average BER is 0.0003 for $\sigma_\upsilon^2 = 0$ dB, while for $\sigma_\upsilon^2 = 2$, 4, 8 dB, the average BER are 0.0004, 0.0005, and 0.0009, respectively.

Figure 13 shows the average BER versus the number of active users (K_u) for different receivers as in Fig. 11 and for SNR = 10 dB, and $\sigma_\upsilon^2 = 4$ dB. At a BER of 10^{-4}, CGBF and MF receiver support $K_u = 101$ users with the BSA-MTP technique, while it can support $K_u = 66$ users with the conventional BSA technique. In addition, the figure shows that the average BER in the CLMS algorithm is higher than that in the CGBF algorithm. Also, we observe that the average BER in the SB technique is lower than that in the CGBF algorithm. For example, at a BER of 10^{-5} and for the BSA-MTP technique, two-stage RAKE receiver support $K_u = 104$ users with the SB technique, while with the CGBF and CLMS algorithms

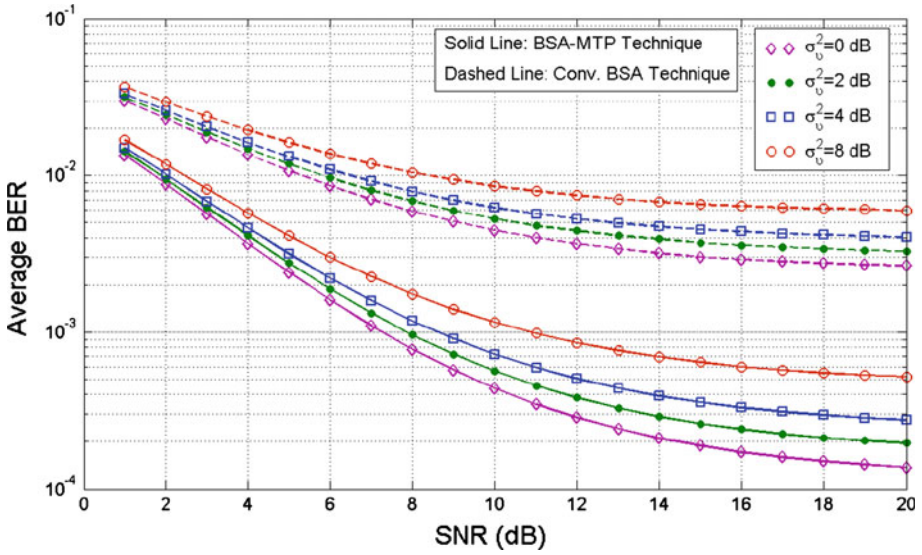

Fig. 12 Average BER versus the SNR for different values of σ_{υ}^2

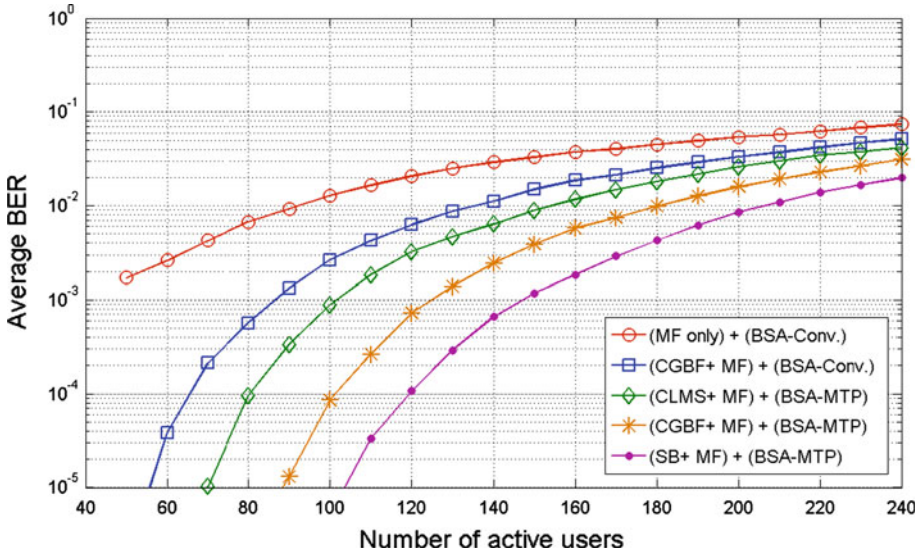

Fig. 13 Average BER versus K_u for $\sigma_{\upsilon}^2 = 4$ dB and SNR $= 10$ dB

it can support $K_u = 89$ and $K_u = 70$ users, respectively. Also, it can be seen that the two-stage RAKE receiver can achieve lower BER than the MF only receiver. It should be mentioned that increasing the number of active users (K_u) will increase the number of users that can be transferred to other base stations (K_r) in BSA-MTP technique.

Figure 14 presents the average BER versus the number of active users as in Fig. 12, for SNR $= 10$ dB and different values of σ_{υ}^2. Similar to our observation in Fig. 12, we observe

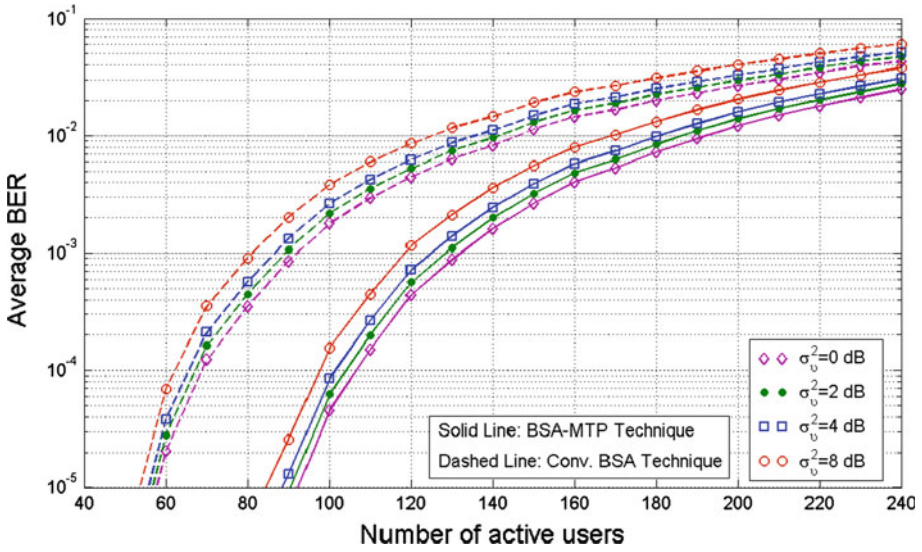

Fig. 14 Average BER versus K_u for different values of σ_υ^2

that the average BER for $\sigma_\upsilon^2 = 0$ dB is lower than $\sigma_\upsilon^2 = 2, 4$, and 8 dB. For example, at a BER of 0.01 and for the BSA-MTP technique, CGBF and MF receiver with $\sigma_\upsilon^2 = 0$ dB support $K_u = 193$ users, while for $\sigma_\upsilon^2 = 2$, 4, and 8dB support $K_u = 186$, 180, and 170 users, respectively. Accordingly, in this case, with σ_υ^2 from 2 to 8 dB, the system capacity degrades from 4 to 12% compared to the case of perfect power control. On the other hand, the figure shows that the average BER for BSA-MTP technique is lower than that for conventional MTP technique. For example, at a BER of 0.001 and $\sigma_\upsilon^2 = 2$ dB, the number of users allowed in the system is $K_u = 129$ users for BSA-MTP technique, while for conventional BSA technique this number is $K_u = 89$ users.

Figure 15 shows the average BER versus the number of active users (K_u) for two-stage receivers (SB, CGBF, and CLMS methods in the first stage of the RAKE receiver), different values of σ_υ^2, the BSA-MTP technique, and SNR = 10 dB. Similar to our observation in Fig. 13, it can be observed that the average BER in the SB technique is less than that in the CGBF and CLMS algorithms. For example, at a BER of 0.001 and for $\sigma_\upsilon^2 = 4$ dB, the number of users allowed in the system is $K_u = 147$ users for SB technique, while for CGBF and CLMS algorithms this number is $K_u = 125$ and $K_u = 102$ users, respectively.

Other results displayed in Figs. 16 and 17 show the influence of channel propagation conditions in USPS (path-loss parameter,L_p, and variance of shadowing, σ_ξ^2) on the average BER for CGBF and MF receiver, the BSA-MTP technique, $\sigma_\upsilon^2 = 4$ dB, and SNR = 10 dB. In Fig. 16, we can observe that, as expected, a decrease in the path-loss parameter entails an increase in the interference and desired signal levels and, therefore, an improvement in system performance using antenna arrays in BSs. For example, at a BER of 0.01, capacity is, respectively, 146, 180, and 200 users for $L_p = 0.5$, 0.05, and 0.01 dB/m. Thus, it is seen that if L_p decreases from 0.5 to 0.01 dB/m, the number of active users increases by approximately 37%. In Fig. 17, it is seen that if σ_ξ^2 increases from 6 to 8 dB, the number of active users decreases by approximately 28% for a required average BER of 0.01, whereas if σ_ξ^2 increases from 4 to 6 dB, the capacity decreases by approximately 18%.

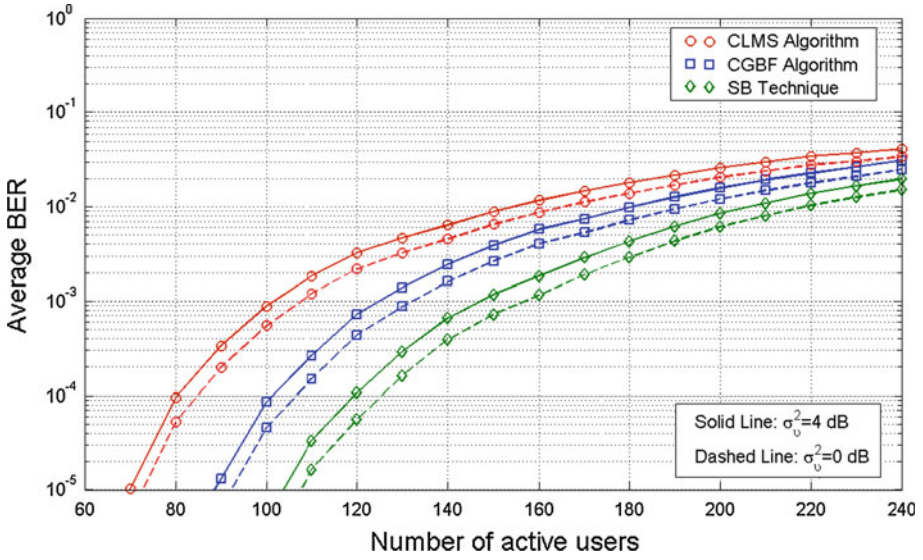

Fig. 15 Average BER versus K_u for the SB, CGBF, and CLMS methods, the BSA-MTP technique, SNR = 10 dB, and for different values of σ_υ^2

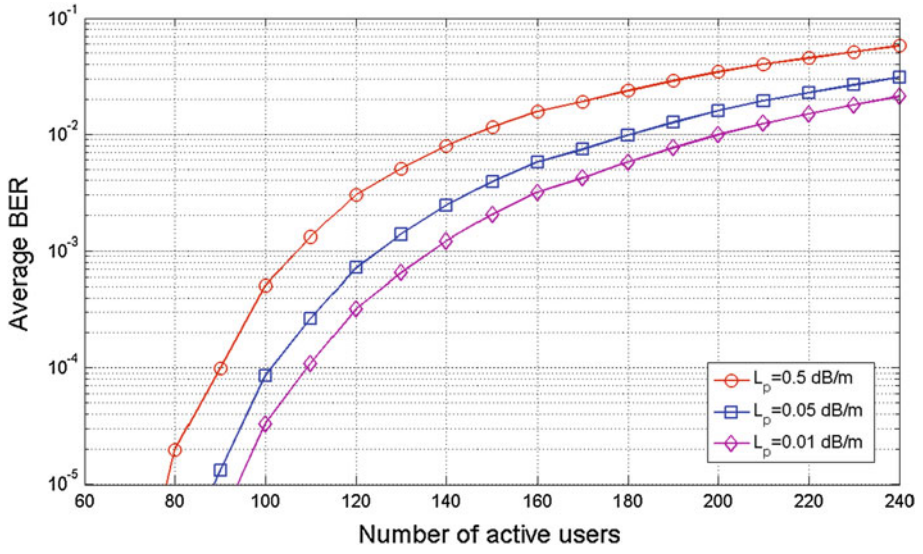

Fig. 16 Influence of path-loss parameter on average BER for the BSA-MTP technique, $\sigma_\upsilon^2 = 4$ dB, and SNR = 10 dB

9 Conclusions

In this paper, we studied the RAKE receiver performance of multiple-cell DS-CDMA system with the space diversity processing, closed-loop power control, base station assignment, and power control error in a 2D urban environment. This receiver consists of two stages. In the first stage, with the CGBF algorithm, the desired users' signal in an arbitrary path is passed

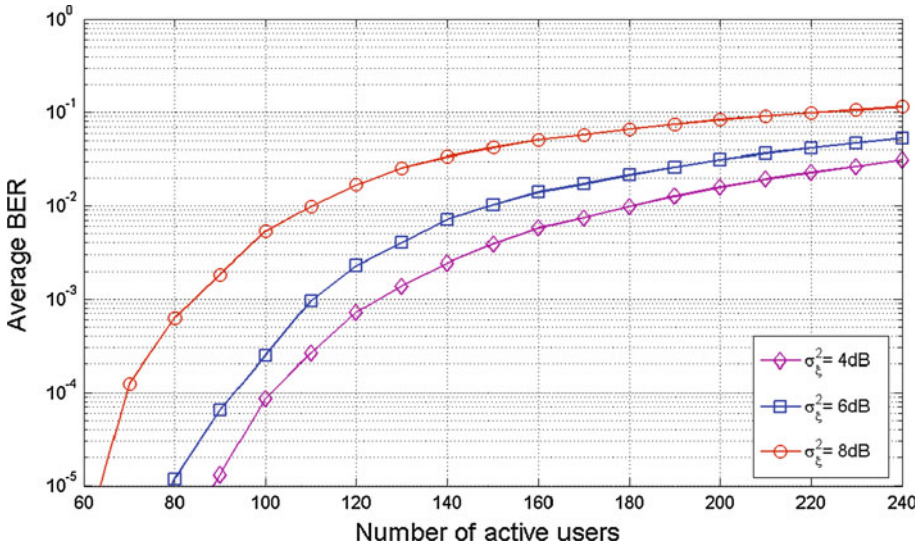

Fig. 17 Influence of variance of shadowing on average BER for the BSA-MTP technique, $\sigma_\upsilon^2 = 4$ dB, and SNR = 10 dB

and the IPI is canceled in other paths in each RAKE finger. Also in this stage, the MAI from other users is reduced. Thus, the MF can be used for more reduction of the MAI in each RAKE finger in the second stage. Finally, the output signals from the MFs are combined and then fed into the decision circuit for the desired user.

Accordingly, we proposed the SSPC algorithm and the BSA-MTP technique to reduce the MAI. It has been shown that, by using antenna arrays at the base stations, the SSPC algorithm and the BSA-MTP technique will decrease the interference in all cells. In addition, it can be seen that the TTP in the SSPC algorithm is less than that in the VSPC and FSPC algorithms. Also, our results show that the TTP for BSA-MTP technique is lower than that in conventional case. Thus, it decreases the BER by allowing the SINR targets for the users to be higher, or by increasing the number of users supportable at a fixed SINR target level. On the other hand, it has been shown that the convergence speed of the SSPC algorithm is increased in comparison with that of the VSPC and FSPC algorithms. In addition, it can be seen that the convergence speed of the joint SSPC algorithm and SB technique is higher than that of the other cases. It has also been observed that using the BSA-MTP technique will decrease the average BER of the system to support a significantly larger number of users. Also, our simulations show that the variations in power level due to PCE have a detrimental effect on system performance.

References

1. Abrardo, A., & Sennati, D. (2000). On the analytical evaluation of closed-loop power-control error statistics in DS-CDMA cellular systems. *IEEE Transactions on Vehicular Technology, 49*(6), 2071–2080.
2. Femenias, G., & Carrasco, L. (2006). Effect of slow power control error on the reverse link of OSTBC DS-CDMA in a cellular system with Nakagami frequency-selective MIMO fading. *IEEE Transactions on Vehicular Technology, 55*(6), 1927–1934.

3. Wang, J. T. (2009). Admission control with distributed joint diversity and power control for wireless networks. *IEEE Transactions on Vehicular Technology, 58*(1), 409–419.
4. Fischione, C., Butussi, M., Johansson, K. H., & D'Angelo, M. (2009). Power and rate control with outage constraints in CDMA wireless networks. *IEEE Transactions on Communications, 57*(8), 2225–2229.
5. Gejji, R. R. (1992). Forward-link-power control in CDMA cellular systems. *IEEE Transactions on Vehicular Technology, 41*(4), 532–536.
6. Carrasco, L., & Femenias, G. (2008). Reverse link performance of a DS-CDMA system with both fast and slow power controlled users. *IEEE Transactions on Wireless Communications, 7*(4), 1255–1263.
7. Qian, L., & Gajic, Z. (2006). Variance minimization stochastic power control in CDMA system. *IEEE Transactions on Wireless Communications, 5*(1), 193–202.
8. Rintamaki, M., Koivo, H., & Hartimo, I. (2004). Adaptive closed-loop power control algorithms for CDMA cellular communication systems. *IEEE Transactions on Vehicular Technology, 53*(6), 1756–1768.
9. Wang, J., & Yu, A. (2001). Open-loop power control error in cellular CDMA overlay systems. *IEEE Journal on Selected Areas in Communications, 19*(7), 1246–1254.
10. Corazza, G. E., De Maio, G., & Vatalaro, F. (1998). CDMA cellular systems performance with fading, shadowing, and imperfect power control. *IEEE Transactions on Vehicular Technology, 47*(2), 450–459.
11. Romero-Jerez, J. M., Tellez-Labao, C., & Diaz-Estrella, A. (2004). Effect of power control imperfections on the reverse link of cellular CDMA networks under multipath fading. *IEEE Transactions on Vehicular Technology, 53*(1), 61–71.
12. Abrardo, A. (2003). Noncoherent MLSE in DS-CDMA wireless systems with antenna arrays. *IEEE Transactions on Vehicular Technology, 52*(6), 1435–1446.
13. Yang, L.-L., & Fang, W. (2009). Performance of distributed-antenna DS-CDMA systems over composite lognormal shadowing and Nakagami-*m*-fading channels. *IEEE Transactions on Vehicular Technology, 58*(6), 2872–2883.
14. Cai, Y., & de Lamare, R. C. (2009). Space-time adaptive MMSE multiuser decision feedback detectors with multiple-feedback interference cancellation for CDMA systems. *IEEE Transactions on Vehicular Technology, 58*(8), 4129–4140.
15. Abdel-Samad, A., Davidson, T. N., & Gershman, A. B. (2006). Robust transmit eigen beamforming based on imperfect channel state information. *IEEE Transactions on Signal Processing, 54*(5), 1596–1609.
16. Wang, J., & Payaro, M. (2010). On the robustness of transmit beamforming. *IEEE Transactions on Signal Processing, 58*(11), 5933–5938.
17. Nai, S. E., Ser, W., Yu, Z. L., & Rahardja, S. (2009). A robust adaptive beamforming framework with beampattern shaping constraints. *IEEE Transactions on Antennas and Propagation, 57*(7), 2198–2203.
18. El-Keyi, A., & Champagne, B. (2010). Adaptive linearly constrained minimum variance beamforming for multiuser cooperative relaying using kalman filter. *IEEE Transactions on Wireless Communications, 9*(2), 641–651.
19. Lorenz, R. G., & Boyd, S. P. (2005). Robust minimum variance beamforming. *IEEE Transactions on Signal Processing, 53*(5), 1684–1696.
20. Lawrence, D. E. (2010). Low probability of intercept antenna array beamforming. *IEEE Transactions on Antennas and Propagation, 58*(9), 2858–2865.
21. Park, S.-H., Lee, H., Lee, S.-R., & Lee, I. (2009). A new beamforming structure based on transmit-MRC for closed-loop MIMO systems. *IEEE Transactions on Communications, 57*(6), 1847–1856.
22. Dosaranian-Moghadam, M., Bakhshi, H., & Dadashzadeh, G. (2010). Interference management for DS-CDMA systems through closed-loop power control, base station assignment, and beamforming. *Journal of Wireless Sensor Network, 2*(6), 472–482.
23. Dosaranian-Moghadam, M., Bakhshi, H., & Dadashzadeh, G. (2010). Adaptive beamforming method based on closed-loop power control for DS-CDMA receiver in multipath fading channel. *21st Annual IEEE International Symposium on Personal, Indoor, and Mobile Radio Communications,* Istanbul, Turkey, pp. 2087–2092, Sep. 26–30.
24. Dosaranian-Moghadam, M., Bakhshi, H., & Dadashzadeh, G. DS-CDMA cellular systems performance with base station assignment, power control error, and beamforming over multipath fading. *International Journal of Computer Networks & Communications* (accepted)
25. Dosaranian-Moghadam M., Bakhshi H., Dadashzadeh G., & Godarzvand-Chegini M. (2010). Joint closed-loop power control and constrained LMS algorithm for DS-CDMA receiver in multipath fading channels. In *Proceedings of 2010 IEEE global mobile congress*, Shanghai, China, pp. 1–8, Oct. 18–19.
26. Dosaranian-Moghadam, M., Bakhshi, H., Dadashzadeh, G., & Godarzvand-Chegini, M. (2010). Joint base station assignment, power control error, and adaptive beamforming for DS-CDMA cellular systems in multipath fading channels. In *Proceedings of 2010 IEEE global mobile congress*, Shanghai, China, pp. 1–7, Oct. 18–19.

27. Mohamed, N. A., & Dunham, J. G. (2002). A low-complexity combined antenna array and interference cancellation DS-CDMA receiver in multipath fading channels. *IEEE Journal on Selected Areas in Communications, 20*(2), 248–256.
28. Mohamed, N. A., & Dunham, J. G. (1999). Adaptive beamforming for DS-CDMA using conjugate gradient algorithm in a multipath fading channel. In *Proceedings of 1999 IEEE emerging technologies symposium*, Dallas, TX, pp. 859–863, Apr. 12–13.
29. Hanly, S. V. (1995). An algorithm for combined cell-site selection and power control to maximize cellular spread spectrum capacity. *IEEE Journal on Selected Areas in Communications, 13*(7), 1332–1340.
30. Dosaranian-Moghadam, M., Bakhshi, H., & Dadashzadeh, G. (2010). Interference management for DS-CDMA receiver through base station assignment in multipath fading channels. In *Proc. 2010 IEEE international conference on wireless communications, networking and information security*, Beijing, China, pp. 257–263.
31. Dosaranian-Moghadam, M., Bakhshi, H., & Dadashzadeh, G. (2010). Joint centralized power control and cell sectoring for interference management in CDMA cellular systems in a 2D urban environment. *Journal of Wireless Sensor Network, 2*(8), 599–605.
32. Dosaranian-Moghadam, M., Bakhshi, H., Dadashzadeh, G., & Rahmati, P. (2009). Adaptive beamforming method based on constrained LMS algorithm for tracking mobile user. In *Proceedings of 2009 IEEE global mobile congress*, Shanghai, China, pp. 1–6.
33. Dosaranian-Moghadam, M., Bakhshi, H., & Dadashzadeh, G. (2010). Reverse link performance of DS-CDMA cellular systems through closed-loop power control and beamforming in 2D urban environment. *International Journal of Computer Networks & Communications, 2*(6), 136–153.
34. Rashid-Farrokhi, F., Ray-Liu, K. J., & Tassiulas, L. (1998). Transmit beamforming and power control for cellular systems. *IEEE Journal on Selected Areas in Communications, 16*(8), 1437–1450.
35. Litva, J., & Kwok-Yeung, T. (1996). *Digital beamforming in wireless communications*. London: Artech-House.
36. Peterson, R. L., Ziemer, R. E., & Borth, D. E. (1995). *Spread-spectrum communications*. Englewood Cliffs: Prentice-Hall.
37. Kong, N., & Milstein, L. B. (1999). Average SNR of a generalized diversity selection combining scheme. *IEEE Communications Letters, 3*(3), 57–59.
38. Yener, A., Yates, R. D., & Ulukus, S. (2001). Interference management for CDMA systems through power control, multiuser detection, and beamforming. *IEEE Transactions on Communications, 49*(7), 1227–1239.
39. Kandukuri, S., & Boyd, S. (2002). Optimal power control in interference-limited fading wireless channels with outage probability specifications. *IEEE Transactions on Wireless Communications, 1*(1), 46–55.
40. Zhang, R., Chai, C. C., & Liang, Y.- C. (2009). Joint beamforming and power control for multiantenna relay broadcast channel with QoS constraints. *IEEE Transactions on Signal Processing, 57*(2), 726–737.
41. Grandhi, S. A., Vijayan, R., Goodman, D. J., & Zander, J. (1993). Centralized power control in cellular radio systems. *IEEE Transactions on Vehicular Technology, 42*(4), 466–468.
42. Zander, J. (1992). Distributed cochannel interference control in cellular radio systems. *IEEE Transactions on Vehicular Technology, 41*(3), 305–311.
43. Kurniawan, A. (2002). Effect of feedback delay on fixed step and variable step power control algorithm in CDMA systems. *IEEE International Conference on Communication Systems, Singapore, 2*, 1096–1100.
44. Liberti, J. C., & Rappaport, T. S. (1999). *Smart antennas for wireless communications IS-95 and third generation CDMA applications*. Englewood Cliffs: Prentice-Hall.
45. Rashid-Farrokhi, F., Tassiulas, L., & Ray-Liu, K. J. (1998). Joint optimal power control and beamforming in wireless networks using antenna arrays. *IEEE Transactions on Communications, 46*(10), 1313–1324.
46. Sun, X. Y., Lian, X. H., & Zhou, J. J. (2008). Robust adaptive beamforming based on maximum likelihood estimation. In *Proceedings of 2008 IEEE international conference on microwave and millimeter wave technology*, Nanjing, China, vol. 3, pp. 1137–1140, Apr. 21–24.
47. Gotsis, K. A., Siakavara, K., & Sahalos, J. N. (2009). On the direction of arrival (DoA) estimation for a switched-beam antenna system using neural networks. *IEEE Transactions on Antennas and Propagation, 57*(5), 1399–1411.

Author Biographies

Mohamad Dosaranian-Moghadam was born in Tehran, Iran on May 26, 1979. He received the B.Sc. degree in electrical engineering from Islamic Azad University of Qazvin, Iran and the M.Sc. degree in communication engineering from Ferdowsi University, Mashad, Iran, in 2002 and 2005, respectively. He is currently working toward the Ph.D. degree in the Department of Electrical Engineering, Science and Research Branch of Islamic Azad University, Tehran, Iran. His research interests include power control, wireless communications, array and statistical signal processing, smart antennas, and adaptive filtering.

Hamidreza Bakhshi was born in Tehran, Iran on April 25, 1971. He received the B.Sc. degree in electrical engineering from Tehran University, Iran in 1992, the M.Sc. and Ph.D. degree in Electrical Engineering from Tarbiat Modarres University, Iran in 1995 and 2001, respectively. Since 2001, he has been as an Assistant Professor of Electrical Engineering at Shahed University, Tehran, Iran. His research interests include wireless communications, multiuser detection, and smart antennas.

Gholamreza Dadashzadeh was born in Urmia, Iran, in 1964. He received the B.Sc. degree in communication engineering from Shiraz University, Shiraz, Iran in 1992 and M.Sc. and Ph.D. degree in communication engineering from Tarbiat Modarres University (TMU), Tehran, Iran, in 1996 and 2002, respectively. From 1998 to 2003, he has worked as head researcher of Smart Antenna for Mobile Communication Systems (SAMCS) and WLAN 802.11 project in radio communications group of Iran Telecomm Research Center (ITRC). From 2004 to 2008, he was dean of Communications Technology Institute (CTI) in ITRC. He is currently as Assistance Professor in the Department of Electrical Engineering at Shahed University, Tehran, Iran. He is a member of IEEE, Institute of Electronics, Information and Communication Engineers (IEICE) of Japan and Iranian Association of Electrical and Electronics Engineers (IAEEE) of Iran. He honored received the first degree of national researcher in 2007 from Iran's ministry of ICT. He has published more than 50 papers in referred journals and international conferences in the area of antenna design and smart antennas.